Research Article | Vol. 11, No. 2 / 1 February 2020 / Biomedical Optics Express 791
Biomedical Optics EXPRESS

Detection of blackbody radiation during fiber guided laser-tissue vaporization

PARIS FRANZ,[1,5] XIAOMEI WANG,[2] HUI ZHU,[3] RAY CHIA,[4] TOM HASENBERG,[4] AND HUI WANG[1,*]

[1]Department of Chemical, Paper and Biomedical Engineering, Miami University, OH 45056, USA
[2]Department of Computer Science, Shanghai Normal University, China
[3]Glickman Urological and Kidney Institute, Cleveland Clinic Foundation, OH 44125, USA
[4]Boston Scientific, MA 01752, USA
[5]Currently with Department of Applied Physics, Stanford University, CA, USA
[*]hui.wang@miamioh.edu

Abstract: Laser-tissue vaporization through a fiber catheter is evolving into a major category of surgical operations to remove diseased tissue. Currently, during a surgery, the surgeon still relies on personal experience to optimize surgical techniques. Monitoring tissue temperature during laser-tissue vaporization would provide important feedback to the surgeon; however, simple and low-cost temperature sensing technology, which can be seamlessly integrated with a fiber catheter, is not available. We propose to monitor tissue temperature during laser-tissue vaporization by detecting blackbody radiation (BBR) between 1.6 µm-1.8 µm, a relatively transparent window for both water and silica fiber. We could detect BBR after passing through a 2-meter silica fiber down to ~70°C using lock-in detection. We further proved the feasibility of the technology through ex vivo tissue studies. We found that the BBR can be correlated to different tissue vaporization levels. The results suggest that this simple and low-cost technology could be used to provide objective feedback for surgeons to maximize laser-tissue vaporization efficiency and ensure the best clinical outcomes.

1. Introduction

Laser-tissue vaporization (LTV) uses a high power laser to quickly heat and vaporize tissue [1]. Usually, the light from the high-power laser is delivered through a fiber catheter to the location of the tissue to be removed. The tissue will be quickly heated to the boiling point of water due to light absorption. The bubbles generated inside of the tissue tear the tissue off, a process called vaporization. LTV has emerged as a new generation of surgical technology to treat different diseases due to its excellent hemostatic capability [2]. In urology, it has been widely embraced to treat Benign prostate hyperplasia (BPH) using a green laser at 532 nm or a Holmium/Thulium laser at 2 µm [3]. Recently, it has also been explored for bladder tumor removal [4,5]. In gynecology, LTV has been employed for treating cervical cancer and vaginal neoplasia [6,7]. Gastroenterologists have used LTV to treat esophageal and rectal cancer [8,9]. In order to achieve desired clinical outcomes, various lasers have been evaluated through *ex vivo*, *in vivo*, and clinical studies to compare tissue removal capability, hemostasis, perioperative complications, and postoperative complications [3,10–12].

Ideally, LTV is expected to remove tissue efficiently with excellent hemostasis and minimal collateral tissue damage, which can reduce hospitalization time and complications [12–14]. For the best clinical outcomes, the surgeons are often trained and required to control the power density over the tissue during surgery by adjusting the distance between the catheter tip and the tissue surface, keeping a constant sweeping speed of the catheter, and closely monitoring the tissue responses to laser vaporization. Usually, an optimal sweeping speed and working distance of the fiber catheter are recommended to surgeons based on *ex vivo* tissue or animal studies [15–19].

#376141 https://doi.org/10.1364/BOE.376141
Journal © 2020 Received 4 Oct 2019; revised 29 Dec 2019; accepted 3 Jan 2020; published 14 Jan 2020

Biomedical Optics EXPRESS

However, all of these surgical techniques are subjective and depend on the experience of the individual surgeon. To our knowledge, no objective feedback has been provided to the surgeon to help them optimize the laser vaporization process and the cognitive load during LTV remains excessive.

Tissue temperature during LTV is the most important parameter for a surgeon to know during a procedure. Tissue cannot be vaporized if the temperature is lower than the boiling point, while high temperatures may lead to carbonization over the tissue surface, which not only reduces vaporization efficiency but also leads to postsurgical complications [20]. However, sensing tissue temperature variation during LTV remains very challenging. Thermocouples and fiber gratings have been used to monitor tissue temperature *ex vivo* [21], but both sensors are invasive and can only monitor temperature at a single location, making them difficult to use in a clinical setting. Additionally, integrating either sensor with a laser vaporization fiber catheter adds to the complexity of the system. In contrast, blackbody radiation (BBR) is a non-invasive thermal sensing technology. It is of special interest that the fiber catheter could be used simultaneously for both vaporization and detection of the BBR for sensing tissue temperature. Usually, the BBR for sensing temperature is detected in the mid-wave (3-5 μm) or long-wave (6-12 μm) infrared range (MWIR and LWIR) as the BBR in short-wave (1-2.5 μm) infrared range (SWIR) is considered too weak to be measured if the measured temperature is not high, e.g. less than 200°C. However, measuring BBR in MWIR and LWIR is not feasible through a fiber catheter. Almost all fiber catheters currently used in clinics are fabricated with silica fiber. The attenuation of silica fiber in MWIR and LWIR is extremely high [22]. BBR in MWIR and LWIR cannot be guided through a silica fiber. Special fibers with a high transmission in MWIR and LWIR have been proposed to solve this issue [23]. However, during LTV, the tissue is usually immersed in saline water. Due to the strong water absorption in MWIR and LWIR, the BBR in this range will be dramatically attenuated [24]. Even if a special fiber could be used for transmitting the BBR in MWIR and LWIR, the extremely high water absorption would make detection in clinical applications very difficult. Till now, to our knowledge, BBR has never been used for temperature sensing during LTV. Currently, magnetic resonance thermometry (MRT) is considered the most successful

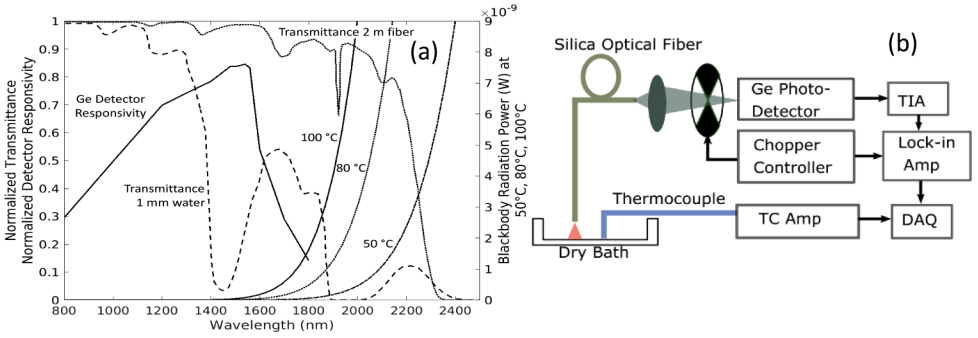

Fig. 1. (a) Both 2-meter silica fiber transmittance and the transmittance through 1 mm water are normalized to the values at 800 nm, a wavelength having very water absorption and high fiber transmittance. The power due to blackbody radiation at three different temperatures were calculated from an 0.17 mm^2 circular area (0.6 mm diameter). The wavelength responsivity curve of a Germanium detector is also plotted. (b) The layout of the bench-top experiment. The BBR from the temperature controlled dry bath was received by a 2 m multimode silica fiber and then modulated by a chopper. The detected current signal from a Ge detector was first amplified through a transimpedance amplifier (TIA) and then demodulated by a lock-in amplifier. Simultaneously, a thermocouple (TC) was used to calibrate the blackbody radiation signal.

Biomedical Optics EXPRESS

technology to monitor tissue temperature in clinics and has been popularly used for sensing temperature during brain surgery. However, MRT is complex, costly, and cannot be realistically used in common and routine LTV, such as BPH surgery [25].

In this paper, we explore the feasibility of detecting the BBR emitted in SWIR to sense tissue temperature variation during LTV. In particular, we want to determine if temperature related BBR variation can be related to the outcome of LVT. As shown in Fig. 1(a), the light transmission of 2-meter silica fiber is above 50% up to 2.2 µm, while a relatively low water absorption band can be identified between 1.6 -1.8 µm. Although BBR below the 1.8 µm is weak, the high transmission of silica fiber and the relatively low water absorption make the BBR in SWIR of interest to sense temperature variation. In addition, popular and low-cost InGaAs and Germanium (Ge) detectors can cover this wavelength range well. As long as the BBR below 1.8 µm can be detected, it may be used as an objective feedback for tissue removal rate, avoiding overheating the tissue (carbonization), and reducing the learning curve for surgeons. In the future, it could also be used as a feedback to develop robotic surgery devices.

2. Experimental setup and methods

2.1. Bench-top setup

A diagram of the bench-top study layout is shown in Fig. 1(b). A temperature controlled dry bath (ThermoFisher) was used to generate BBR in the temperature range of 50°C to 110°C and Scotch Super 33++ black tape was used to cover the reflective dry bath surface to increase the emissivity. A 2-meter low-OH silica fiber with a diameter of 600 µm and numerical aperture 0.5 (Thorlabs M53L02) was mounted on a translational stage with the tip perpendicular to the surface of the dry bath to receive BBR. The BBR from the fiber output was focused by a lens (Thorlabs AC254-030-B-ML), then the focused beam passed through an optical chopper (Stanford Research Systems Model SR540) into a Ge biased detector (Thorlabs DET30B2). The BBR was modulated at 270 Hz. The signal was amplified by a transimpedence amplifier (ILX Lightwave PDA-6424) and then demodulated by a lock-in amplifier (Eg&G Princeton Applied Research Model 5104) with a time constant of 1s and recorded using a myDAQ (National Instruments). A T-type thermocouple (Marlin) was used with a thermocouple amplifier with cold-junction compensation (National Instruments USB-TC01) to record the surface temperature of the dry bath. A LabVIEW (National Instruments) code was developed to simultaneously record the signal from the fiber and the thermocouple.

2.2. Ex vivo tissue vaporization setup

Porcine kidney tissue was obtained from a slaughterhouse and delivered overnight immediately after scarifying. All studies were completed within 8 hours after receiving the tissue. The kidneys were dissected into pieces of size 25 mm ×25mm×10 mm. All tissue pieces were kept in saline to prevent dehydration. During laser vaporization, each tissue piece was fixed in a custom-made tissue holder with the cortex side exposed to the laser through a 10 mm × 10 mm window as shown in Fig. 2.

The laser used in this study was the GreenLight XPS^{TM} (Boston Scientific) system. During the study, the laser power was set at 120 W and delivered through a commercial surgical fiber catheter, MoXy^{TM} Liquid-Cooled Fiber (Boston Scientific), which has a diameter of 650 µm. The MoXy fiber is a side-firing fiber, which can deflect the laser beam by 75°, with a beam acceptance angle of ~8° measured in water. During the study, the fiber tip was tilted to 15° to make sure that the laser beam perpendicularly illuminated the surface of a tissue sample. The tissue holder was set on a motor-controlled translational stage, whose speed can be controlled from 1 mm/s to 30 mm/s. The working distance from the laser beam emission window to the surface of the tissue sample was set at 2.5 mm. A continuous saline flow at 5.6 ml/s was directed onto the fiber tip

Biomedical Optics EXPRESS

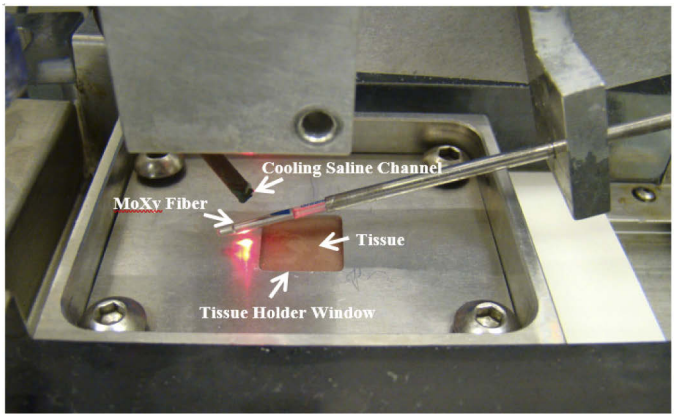

Fig. 2. The setup for *ex vivo* laser vaporization using porcine kidney tissue. The arrows mark the fiber, the tissue sample, cooling saline channel, and the window for exposing the tissue to the laser.

and the tissue surface to flush away the tissue debris during vaporization and cool the fiber tip through a cooling channel as shown in Fig. 2. This flow rate is similar to the saline flow rate used in clinics using a cystoscope. A photo of the setup is shown in Fig. 2.

2.3. Tissue vaporization

To create tissue vaporization at different vaporization levels, tissue samples were controlled to pass through the laser beam at different speeds by the translational stage. Due to different dwelling durations of the laser beam at each point of the tissue sample, the radiant exposure (J/cm^2) over the sample was different, resulting in different levels of tissue vaporization. The translational speed can be thought of as similar to the sweeping speed of the fiber catheter tip during a clinical procedure. During the studies, the laser was turned on before reaching the tissue sample and then turned off after passing the right edge of the tissue holder window. The MoXy fiber simultaneously delivered high power laser to a tissue sample and collected the BBR from the tissue. The BBR was recorded every 0.25 second, which is the set sampling rate of the Greenlight XPS.

2.4. Tissue and data processing

After vaporization, each tissue sample was cut into 10 slices with a thickness of ~ 1 mm. We only used three slices from the middle part of each tissue sample to ensure the working distances during vaporization were similar. At each radiant exposure or translational speed, we conducted tissue vaporization on six tissue samples from three different kidneys. The tissue slices were then immersed in 2% 2,3,5-triphenyltetrazolium chloride (TTC; Sigma-Aldrich) for 20 minutes at room temperature for staining. Each slice was photographed and the depths and the areas of the vaporized cavities were manually measured using ImageJ (National Institutes of Health). The tissue volume removal rate was calculated by multiplying the area of the vaporized area with the tissue sample translational speed.

3. Results and discussion

3.1. Blackbody radiation measurement through the bench-top setup

We first quantified the relation between the temperature and the BBR through the bench-top studies. A voltage signal proportional to the BBR was measured every 0.2 s with the fiber tip

Biomedical Optics EXPRESS

2 mm above the dry bath surface. The surface was first heated and then cooled over a temperature range of 50-109°C, which was measured simultaneously by a thermocouple in contact with the surface. Two heating and two cooling cycles were recorded. The lock-in amplifier time constant was set at 1 s, and the BBR signal was sampled every 0.2 s. We also applied a central moving average to the data over windows of 1 s to remove the high frequency electronic noise. The signal from the four cycles were averaged and plotted in Fig. 3(a). The relation between the BBR signal and the temperature can be fit using a power function, and sensitivity was calculated by taking the derivative of the fitted line as shown in Fig. 3(a).

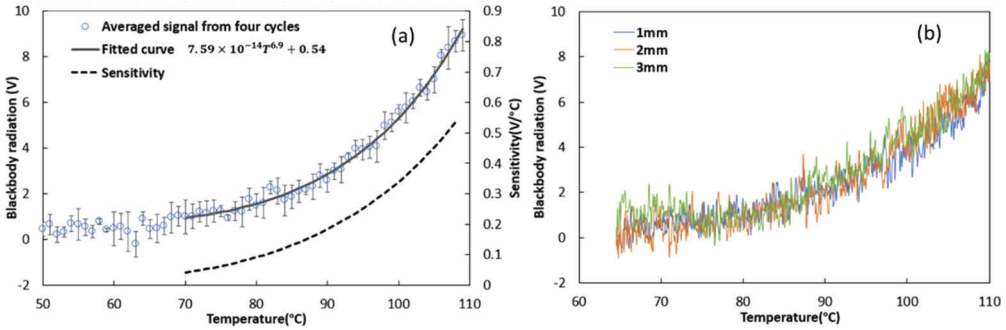

Fig. 3. (a). Average BBR signal measurement is shown with standard deviation error bars. The measured BBR was fitted with a power function, and the sensitivity was found by taking the derivative of the fit. The data is only shown every degree for clarity; (b) Blackbody radiation measured at different working distances, 1 mm, 2 mm, and 3 mm between 65°C and 110 °C.

Figure 3 shows that our setup can sense temperatures down to ~70°C, where the signal is close to the noise floor. The measured BBR has a nonlinear relation with temperature due to the nonlinear relation given by Stefan's Law. Thus, the measurement has a higher sensitivity at a higher temperature and a lower sensitivity at a lower temperature. The data suggests that it is possible to monitor tissue temperature during LTV in SWIR below 1.8 µm through a silica fiber. The temperature during LTV is usually above 100°C.

3.2. Blackbody radiation measurement at different working distances

During LTV, the surgeon often needs to maintain a working distance between the fiber tip and the tissue surface to prevent tissue debris from sticking to the surface of the fiber tip, which could lead to the fiber tip overheating. Additionally, the surgeon can adjust the radiant exposure over the tissue by changing the working distance. However, determining and controlling an optimal working distance relies completely on the experience of each individual surgeon. Therefore, it is important to quantify the BBR due to temperature at different working distances. Theoretically, BBR is independent of the working distance and the angle between the fiber and the tissue surface, but proportional to the numerical aperture and the fiber diameter [26]. We measured the BBR over a temperature range of 65-110 °C with the fiber tip positioned at 1, 2, and 3 mm above the dry bath surface. As shown in Fig. 3(b) the BBR signals measured at the different distances are almost independent of the working distance.

3.3. Blackbody radiation during LTV

The bench-top study demonstrated the feasibility of detecting BBR at temperatures above ~70 °C within a transparent wavelength window in SWIR for both silica fiber and water. It is important to further prove the feasibility of using this technology during LTV. Figure 4 shows the measured BBR during LTV at three different radiant exposures that were achieved by translating a tissue

Biomedical Optics EXPRESS

sample at different speeds under a laser beam. The signals shown in the red boxes in Fig. 4(a)-(c) are the detected BBR signal related to the tissue temperature. We ignored the signal around the initial and the end period of the scanning due to potential artifacts introduced by the edges of the metal window of the tissue holder, as shown by the high peaks in Fig. 4. (b) and (c). The photos are the tissue surficial appearances after vaporization. As the MoXy fiber was continually cooled by saline at 25°C, the BBR from the fiber catheter is negligible.

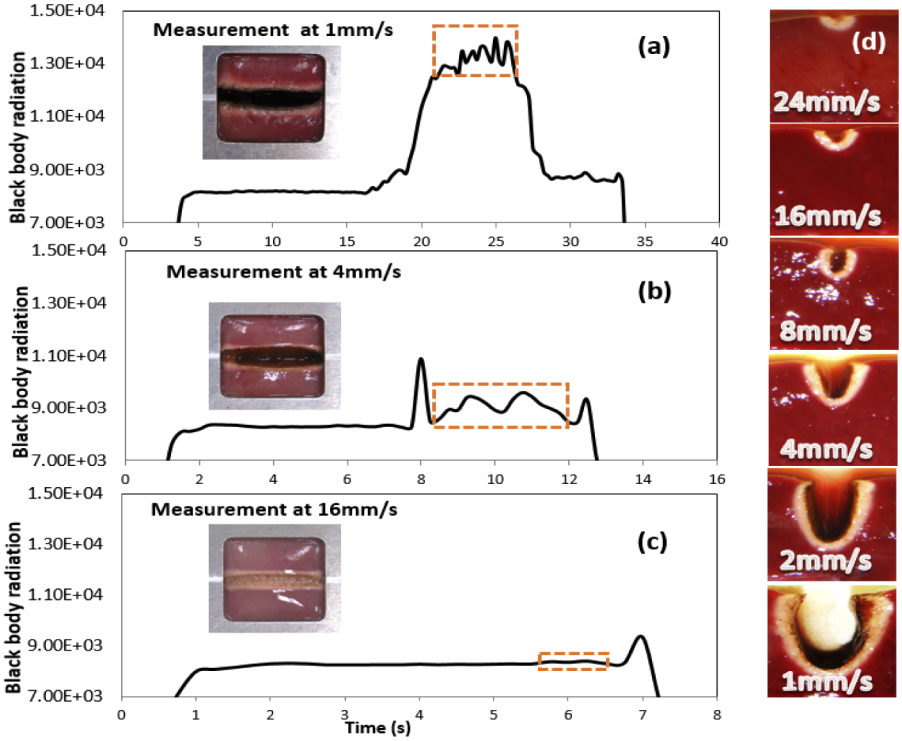

Fig. 4. Blackbody radiation measured during LTV. Three typical cases at different vaporization levels were shown as (a)-(c). The red boxes indicate the detected BBR signals by excluding the signals at the edges of the tissue holder window. The inset photos were taken immediately after vaporization to show the appearances of the tissue samples. (d) The vaporized cavities at different translation speeds. Tissue samples were immediately removed from the tissue sample holder and then stained with TTC to enhance the contrast of the coagulated layer.

Figure 4(d) shows the cross-sectional images of the vaporized cavities at different radiant exposures. For the minimal radiant exposure at a scanning speed of 24 mm/s, tissue vaporization can be barely observed except for a white coagulated layer. We also did not detect BBR signal at this speed. With increasing radiant exposures, the tissue vaporization gradually increased (Fig. 4(d)). We were able to detect BBR signal when the translational speed was less than 16 mm/s, which also resulted in visible vaporization cavities. Carbonized layers are clearly visible over the cavities created at 2 mm/s and 1 mm/s. With TCC staining, the boundaries of the coagulated layers can also be clearly visualized.

Biomedical Optics EXPRESS

3.4. Quantifying the relations between radiant exposure, BBR, and tissue volume removal rate

We first calculated the mean value of the BBR in the red boxes shown in Fig. 4(a)-(c) at different tissue sample translational speeds and plotted them in Fig. 5. The translational speed is inversely proportional to the radiant exposures. Clearly, a higher radiant exposure leads to higher BBR signal, indicating the tissue surface temperature became higher. When the tissue surficial temperature was very high, a carbonized layer was formed over the cavity as shown in Fig. 5 at 2 mm/s and 1 mm/s with the radiant exposure values above 30 J/mm^2. Figure 5 also shows that the relationship between the BBR signal and different radiant exposures is not linear. It should be noted that the tissue samples were immersed in saline, so the BBR signal was detected through a 2.5 mm water layer and a 2-meter MoXy fiber. We cannot detect signal at 24 mm/s when vaporization is not significant. Carbonization could also contribute to BBR detection due to the change of tissue BBR emissivity. In previous study [27], such change was considered minimal when BBR was detected in infrared range (IR). In this study, BBR was detected in near infrared (NIR) range. The absorption of tissue in NIR is less than that in IR, so emissivity with carbonization could be increased more. Increased emissivity makes the detection of overheating (serious carbonization) easier.

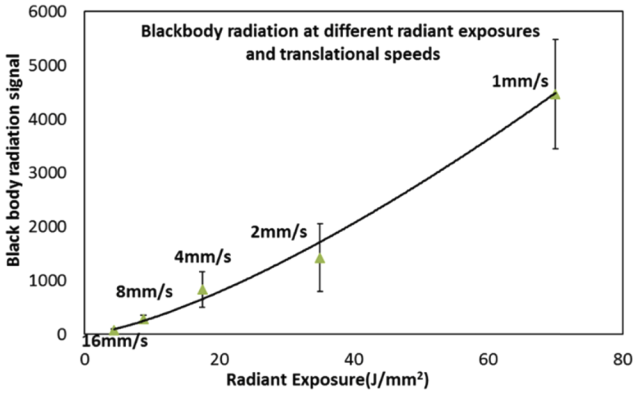

Fig. 5. Blackbody radiation averaged from the values in the red boxes shown in Fig. 4(a)-(c).

During LTV, it is important to remove tissue quickly and cleanly with minimal complications. The depths of the vaporized cavities and the tissue volume removal rates at different translational speeds were plotted in Fig. 6. The depths were measured from the center of the opening of a cavity to the center of the bottom of the cavity. Higher radiant exposures achieved by a slower translational speed created deeper cavities, but the relationship between them is also nonlinear. In contrast, volumetric tissue removal rate (mm^3/s) shows a different trend. Although the largest cavity was created at 1 mm/s, the tissue volume removal rate was not the highest. The maximum volume removal rate was around 35 J/mm^2 or a sweeping speed at around 2 mm/s for our case. The reduced tissue removal rate at 1 mm/s is due to the formation of a black carbonized layer, which can absorb most of the light and prevent light from penetrating to the tissue below it.

Apparently, in clinics, we desire to control the radiant exposure between 17J/mm^2 and 35 J/mm^2 to maximize tissue removal rate without significant overheating (carbonization). However, in current clinics, surgeons try to optimize the radiant exposure to remove tissue as fast as possible by controlling sweeping speed, working distance, and laser power. The clinical outcomes depend mainly on the surgeon's personal experience and require extensive training as no objective feedback is available to guide LTV. From Fig. 6, for our configuration, we can identify the optimal sweeping speed/radiant exposure, which results in maximum tissue volume removal

Biomedical Optics EXPRESS

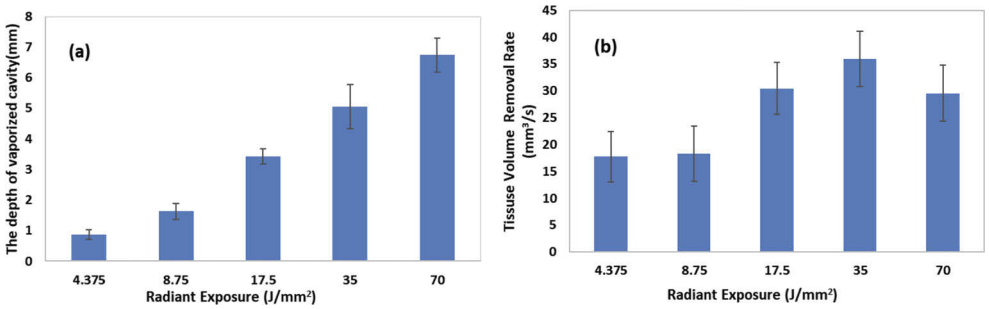

Fig. 6. (a) The depths of vaporized cavities at different radiant exposures; (b) The tissue volume removed at different radiant exposures. The tissue volume removed was calculated by multiplying the vaporized area with the translational speed. The radiant exposure was calculated from the translational speed and the power density.

rate without a significant carbonized layer. At the optimal radiant exposure (sweeping speed at ~ 2-3 mm/s), BBR signal under 1.8 µm is detectable even after passing through 2-meter silica fiber and 2.5 mm water layer and can be differentiated from the BBR signals which did not create sufficient vaporization level (i.e. 8 mm/s) and which overheated the tissue (i.e. 1 mm/s). Therefore, it is promising to employ BBR as an objective feedback to optimize LTV instead of relying on subjective surgeon experience. We believe that an objective feedback for LVT is important not only for surgeons but also for paving the way to develop robotic surgery devices.

As this is a feasibility study to determine if we can relate the degree of LTV to the BBR received through a silica fiber below 1.8 µm, several critical improvements should be done in the future before clinical adoption. Although in the bench-top study we demonstrated that we can detect the BBR above ~70°C, this does not mean that in the *ex vivo* tissue study we were able to sense tissue temperature down to ~70°C. There was a 2.5 mm water layer between the fiber tip and the tissue surface during the tissue study to simulate the clinical setting. The water absorption can reduce the BBR signal between 1.7 µm to 1.8 µm by ~50% per mm as shown in Fig. 1(a). In addition, the N.A. of the MoXy fiber is smaller than the N.A. of the fiber used in the bench study. Therefore, the BBR signal during the tissue study was likely much weaker than that of the bench-top study. It seems that only signal from significant vaporization (>100°C) could be detected. In addition, we cannot solely rely on the BBR signal strength to determine the degree of LVT as it may be affected by many factors, such as the scattering of the tissue debris during LVT or the thickness variation of the water layer. However, it is possible to simultaneously detect BBR signal at two different wavelength ranges, such as one signal at ~1.7 µm and another signal at ~1.8 µm. Instead of using the BBR signal strength, we can use the ratio of the BBR signal strength between two different wavelengths to determine the tissue temperature [28]. The signal we captured in the studies is still noisy, so it is essential to further improve the signal to noise ratio (SNR). In this study, the photodetector worked at room temperature. The sensitivity can be improved by using a cooled photodetector. In addition, we can also detect BBR in parallel with an array, such as a 100 ×100 detector array, which should theoretically improve SNR by 20 dB.

4. Conclusion

Tissue temperature is the most critical parameter that should be monitored during LTV as it can provide real-time objective feedback to surgeons in order to optimize the clinical outcomes. However, technology for *in vivo* temperature sensing during LTV is not yet available due to either high cost or significantly increased complexity for integration. In this paper, we proposed to sense tissue temperature variation by detecting the BBR in SWIR between 1.6- 1.8 µm, which is

Biomedical Optics EXPRESS

a relatively transparent window for both water and silica fiber. We proved the feasibility through bench-top and *ex vivo* tissue studies. In the bench-top study, we showed that at temperatures above 70°C BBR could be detected through a 2-meter silica fiber and the BBR detection was independent of working distance. In the *ex vivo* tissue study, we showed that the BBR has a monotonically increasing relation with vaporization levels, which is related to the volumetric tissue removal rate. The proposed technology is simple, low-cost and can be seamlessly integrated with the fiber catheter already used in LTV. Translating this technology into clinics is highly feasible. However, in the *ex vivo* tissue study, we were unable to determine the absolute tissue temperature as the absolute value of the BBR for a specific temperature is related to tissue emissivity, the length of the fiber catheter, the spectral response of the detector, and the gain of the amplifier. To effectively use this technology for a specific surgical configuration, BBR can be calibrated to the best vaporization level through *ex vivo* or *in vivo* studies, even the exact tissue temperature is unknown. Real-time feedback could be provided to surgeons by displaying a range of the BBR values required for the optimal vaporization level, which the surgeons would aim to achieve during surgery. In an advanced system, the BBR value range could be used as a feedback to automatically control radiant exposure to the optimal vaporization level regardless of the working distance, sweeping speed, or laser power density.

Disclosures

HW, RC, TH: Boston Scientific (P)

References

1. S. Thomsen, "Pathologic Analysis of Photothermal and Photomechanical Effects of Laser–Tissue Interactions," Photochem. Photobiol. **53**(6), 825–835 (1991).
2. S. M. Nair, M. A. Pimentel, and P. J. Gilling, "A Review of Laser Treatment for Symptomatic BPH (Benign Prostatic Hyperplasia)," Curr. Urol. Rep. **17**(6), 45 (2016).
3. X. Zhang, P. Shen, Q. He, X. Yin, Z. Chen, H. Gui, K. Shu, Q. Tang, Y. Yang, X. Pan, J. Wang, N. Chen, and H. Zeng, "Different lasers in the treatment of benign prostatic hyperplasia: a network meta-analysis," Sci. Rep. **6**(1), 23503 (2016).
4. M. Jønler, L. Lund, and S. Bisballe, "Holmium:YAG laser vaporization of recurrent papillary tumours of the bladder under local anaesthesia," BJU Int. **94**(3), 322–325 (2004).
5. M. W. Kramer, T. Bach, M. Wolters, F. Imkamp, A. J. Gross, M. A. Kuczyk, A. S. Merseburger, and T. R. W. Herrmann, "Current evidence for transurethral laser therapy of non-muscle invasive bladder cancer," World J. Urol. **29**(4), 433–442 (2011).
6. M. F. Mitchell, G. Tortolero-Luna, E. Cook, L. Whittaker, H. Rhodes-Morris, and E. Silva, "A randomized clinical trial of cryotherapy, laser vaporization, and loop electrosurgical excision for treatment of squamous intraepithelial lesions of the cervix," Obstet. Gynecol. **92**(5), 737–744 (1998).
7. M. Perrotta, C. E. Marchitelli, A. F. Velazco, P. Tauscher, G. Lopez, and M. S. Perematteu, "Use of CO2 Laser Vaporization for the Treatment of High-Grade Vaginal Intraepithelial Neoplasia," J. Low. Genit. Tract Dis. **17**(1), 23–27 (2013).
8. R. P. Kiran, N. Pokala, and P. Burgess, "Use of laser for rectal lesions in poor-risk patients," Am. J. Surg. **188**(6), 708–713 (2004).
9. J. Oxenberg, S. N. Hochwald, and S. Nurkin, "Ablative Therapies for Colorectal Polyps and Malignancy," https://www.hindawi.com/journals/bmri/2014/986352/.
10. D. S. Elterman, "How I Do It: GreenLight XPS 180W photoselective vaporization of the prostate," Can. J. Urol. **22**(3), 7836–7843 (2015).
11. K. S. Kim, J. B. Choi, W. J. Bae, S. J. Kim, H. J. Cho, S.-H. Hong, J. Y. Lee, S. H. Kim, H. W. Kim, S. Y. Cho, and S. W. Kim, "Comparison of Photoselective Vaporization versus Holmium Laser Enucleation for Treatment of Benign Prostate Hyperplasia in a Small Prostate Volume," PLoS One **11**(5), e0156133 (2016).
12. C. Pascoe, D. Ow, M. Perera, H. H. Woo, G. Jack, and N. Lawrentschuk, "Optimising patient outcomes with photoselective vaporization of the prostate (PVP): a review," Transl. Androl. Urol. **6**(S2), S133–S141 (2017).
13. A. Bachmann, A. Tubaro, N. Barber, F. d'Ancona, G. Muir, U. Witzsch, M.-O. Grimm, J. Benejam, J.-U. Stolzenburg, A. Riddick, S. Pahernik, H. Roelink, F. Ameye, C. Saussine, F. Bruyère, W. Loidl, T. Larner, N.-K. Gogoi, R. Hindley, R. Muschter, A. Thorpe, N. Shrotri, S. Graham, M. Hamann, K. Miller, M. Schostak, C. Capitán, H. Knispel, and J. A. Thomas, "180-W XPS GreenLight laser vaporisation versus transurethral resection of the prostate for the treatment of benign prostatic obstruction: 6-month safety and efficacy results of a European Multicentre Randomised Trial–the GOLIATH study," Eur. Urol. **65**(5), 931–942 (2014).

Biomedical Optics EXPRESS

14. J. A. Thomas, A. Tubaro, N. Barber, F. d'Ancona, G. Muir, U. Witzsch, M.-O. Grimm, J. Benejam, J.-U. Stolzenburg, A. Riddick, S. Pahernik, H. Roelink, F. Ameye, C. Saussine, F. Bruyère, W. Loidl, T. Larner, N.-K. Gogoi, R. Hindley, R. Muschter, A. Thorpe, N. Shrotri, S. Graham, M. Hamann, K. Miller, M. Schostak, C. Capitán, H. Knispel, and A. Bachmann, "A Multicenter Randomized Noninferiority Trial Comparing GreenLight-XPS Laser Vaporization of the Prostate and Transurethral Resection of the Prostate for the Treatment of Benign Prostatic Obstruction: Two-yr Outcomes of the GOLIATH Study," Eur. Urol. **69**(1), 94–102 (2016).
15. W. J. Ko, B. B. Choi, H. W. Kang, D. Rajabhandharaks, M. Rutman, and E. C. Osterberg, "Defining Optimal Laser-Fiber Sweeping Angle for Effective Tissue Vaporization Using 180 W 532 nm Lithium Triborate Laser," J Endourol. **26**(4), 313–317 (2012).
16. J. Oh, S. Y. Nam, Y. W. Lee, and H. W. Kang, "Effect of multiple-sweeping on ablation performance during ex vivo laser nephrectomy," Lasers Surg. Med. **48**(6), 616–623 (2016).
17. H. W. Kang, "Characterization on ablation performance of various surgical fibers," Lasers Med Sci **29**(1), 273–277 (2014).
18. C. Welliver, S. Helo, and K. T. McVary, "Technique considerations and complication management in transurethral resection of the prostate and photoselective vaporization of the prostate," Transl. Androl. Urol. **6**(4), 695–703 (2017).
19. E. Heinrich, F. Schiefelbein, and G. Schoen, "Technique and Short-Term Outcome of Green Light Laser (KTP, 80W) Vaporisation of the Prostate," Eur. Urol. **52**(6), 1632–1637 (2007).
20. J. Manni, *Basic Aspects of Medical and Dental Lasers, P2-32* (Lulu Publishing Service, 2013).
21. E. Schena, D. Tosi, P. Saccomandi, E. Lewis, and T. Kim, "Fiber Optic Sensors for Temperature Monitoring during Thermal Treatments: An Overview," Sensors **16**(7), 1144 (2016).
22. T. Izawa, N. Shibata, and A. Takeda, "Optical attenuation in pure and doped fused silica in the ir wavelength region," Appl. Phys. Lett. **31**(1), 33–35 (1977).
23. G. Tao, H. Ebendorff-Heidepriem, A. M. Stolyarov, S. Danto, J. V. Badding, Y. Fink, J. Ballato, and A. F. Abouraddy, "Infrared fibers," Adv. Opt. Photonics **7**(2), 379–458 (2015).
24. "Optical Absorption of Water Compendium," https://omlc.org/spectra/water/abs/index.html.
25. V. Rieke and K. B. Pauly, "MR Thermometry," Cigongzhen Chengxiang **27**(2), 376–390 (2008).
26. A. Zur and A. Katzir, "Fibers for low-temperature radiometric measurements," Appl. Opt. **26**(7), 1201–1206 (1987).
27. J. Steketee, "Spectral emissivity of skin and pericardium," Phys. Med. Biol. **18**(5), 307686 (1973).
28. A. Hijazi, S. Sachidanandan, R. Singh, and V. Madhavan, "A calibrated dual-wavelength infrared thermometry approach with non-greybody compensation for machining temperature measurements," Meas. Sci. Technol. **22**(2), 025106 (2011).